

June 1985

LRP 264/85

**"AFCO", AN AMPLITUDE AND FREQUENCY CONTROLLED
OSCILLATOR FOR ALFVEN WAVE HEATING (AWH) IN TCA**

A. Lietti and G. Besson

**"AFCO", AN AMPLITUDE AND FREQUENCY CONTROLLED OSCILLATOR
FOR ALFVEN WAVE HEATING (AWH) IN TCA.**

A. Lietti and G. Besson

Centre de Recherches en Physique des Plasmas
Association Euratom - Confédération Suisse
Ecole Polytechnique Fédérale de Lausanne
CH-1007 Lausanne/Switzerland

Abstract

The new rf system for the Lausanne Tokamak TCA experiment is described. The generator operates from 0.3 to 5 MHz and can transfer 1 MW to the plasma for 120 ms in the AWH range. The frequency and the amplitude of the pulse are pre-programmed, an optional feedback control is proposed. Furthermore the paper discusses the method of estimating the rf energy transferred to the plasma. A short comment follows concerning some technical problems of AWH in large size tokamaks.

1. INTRODUCTION

Nowadays AWH in tokamak experiments attracts growing interest both in theory and in experiment. From an engineering point of view this technique is attractive because the frequency range used permits a simple and economical installation. TCA is a medium size tokamak in operation since 1980, and various experimental results have been reported. A recent summary of this work is given by Collins et al. (1985). AWH studies in TCA have been performed until now using a simple self-oscillating device. This apparatus was described by Lietti et al. (1981), some technical problems were further discussed by De Chambrier et al. (1982 a). In principle, this generator produces a pulse of constant amplitude and frequency. Note that the propagation of the Alfvén wave in the plasma changes with the plasma density, which is not constant during the tokamak discharge. For that reason, when we started to design a new more powerful generator, we decided to introduce a control of the frequency and of the amplitude as a function of time.

The idea has been to furnish a device offering a maximum of flexibility, to perform a number of rf experiments in more extended and better controlled condition. In fact the apparatus covers a frequency range even beyond the lower limit of the AWH scheme.

The principal aim of TCA remains, however, the study of AWH, therefore we begin by discussing some aspects of this technique.

2. THE TECHNIQUE OF AWH

2.1 The frequency of operation

The following simplified model describes the AWH principle.

A suitable helical winding in the tokamak chamber produces a compressional collective mode. This kink-like, surface wave introduces the energy in the direction of the minor plasma radius. This wave is converted to a shear Alfvén wave at an inner resonant layer, thus producing an energy flow in the toroidal direction. The frequency which is necessary for this heating method must satisfy the following conditions

$$\omega^2 = \frac{B^2 n^2 (1 + m/nq)^2}{\mu_0 \rho R^2} ; \frac{\omega}{\omega_{ci}} \ll 1 \quad (1)$$

where n and m are the toroidal and poloidal wavenumber. Note that q and ρ are functions of minor radius a . It follows that we should choose a frequency such that the resonant layer is located in the central region.

In TCA the major and minor plasma radii are $R=0,61$ m, $r=0,18$ m, and the electron axial density ranges from 10^{19} to 10^{20} m^{-3} . Experiments have been performed with a toroidal magnetic field ranging from 0,6 to 1,5 T and a plasma current up to 135 KA. The energy absorption as expected from the simplified model was generally observed, both as continuum spectrum and resonance peaks. In addition a Discrete Alfvén Wave spectrum -DAW- was discovered (De Chambrier et al. 1982 b) and the theoretical model improved (Appert et al. 1982). Note that these

experiments were performed at the fixed frequency of 2.5 MHz, and the loading spectrum was observed by varying the density, as figure 1 shows. The new generator will offer the possibility of changing the frequency. The frequencies of major interest for the study of AWH range from 2 to 5 MHz, below the ion-cyclotron frequency, typically $\omega/\omega_{ci} = 0,1-0,3$.

2.2 The antennae configuration

We reported that theory demands an helical winding; the TCA experiment, however, uses a solution which is mechanically more simple. Moreover, the electrical field that is produced by this antenna is considerably lower than the field produced by an equivalent helical antenna, and the electric field component parallel to the magnetic field is strongly reduced. As figure 2 shows, four antenna arrays are situated 90° apart around the torus in the toroidal direction.

Each array consists of two antennae, above and below the plasma. Each antenna is made of six stainless steel bars, connected in parallel. Different modes of excitation are obtained by correctly phasing the antenna currents.

Consider now the electrical equivalent circuit of the antenna. Each antenna is represented by an inductance L_a in series with a resistance r . The inductance results from the mechanical design of the antenna, with only a very little change due to the plasma coupling. The resistance results from the plasma coupling plus some additional loss. The coupling is dependent on the excitation, structure and

changes during the experiment as a result of the density variations.

Large variations of the load are indeed shown in figure 1 and this raises a difficult problem of matching. That shows the importance of having available a circuit able to withstand large reflections.

Consider now the reference load which takes place in the "standard" experimental condition, when the antennae are excited with the $N=2$, $M=|1|$ mode and the continuum spectrum is taken into account. This reference load r_0 is proportional to the frequency, and takes the value of about 100 m Ω for each antenna at 2.5 MHz. The ratio $Q_0=\omega L/r_0=15$ is therefore frequency independent. (L is the inductance of the antenna, as measured at the feedthrough of the vessel.) The non dimensional quantity Q_0 is the reference quality factor of the antenna and its technical relevance is discussed below.

2.3 The frequency excursion

We presented AFCO as a generator covering a large band and frequency controlled. In fact the apparatus is provided with interchangeable units, each to cover a fraction of the operational range and to tune at the centre frequency for the experiment in programme. The apparatus is provided with a control input, driven by an external signal, which produces a frequency shift $\Delta\omega$ during the tokamak discharge. We want to discuss briefly the possible limit of $\Delta\omega$, in circuits carrying large power. In order to avoid excessive losses, the standard rf power technique uses resonant circuits. This way the generator produces only the real power, since the resonant capacitor compensate for the energy of the magnetic field.

If we resonate the antenna with a capacitor, the circuit, considering the connecting leads, will have a quality factor $Q > Q_0$, Q_0 being the factor introduced in § 2.2. In order to maintain the resonant condition during the excursion $\Delta\omega$ it would be necessary to use a variable element (capacitor or inductor). Mechanical solutions are too slow for the TCA experiment. Some preliminary study was undertaken to consider the use of a saturable inductor, but until now no solution was found since the space near the tokamak was not sufficient. A simpler solution was therefore necessary.

A reasonable excursion $\Delta\omega$ is still possible using constant components by properly damping the circuits. This way, only part of the reactive energy is compensated, but the power available still allows the high power experiment foreseen. This view is supported by an elementary estimate. Considering the well known relation of the resonant circuit between the frequency band and the quality factor

$$Q \frac{\Delta\omega}{\omega} = 1 \quad (2)$$

we find that the resonant antenna circuit ($Q=Q_a=15$) allows a frequency excursion $\Delta\omega/\omega=0,066$.

Additional damping results in a broader band, at the expense of the power W_{p1} transferred to the plasma, since it is easy to see that, given a constant power generator, the product $W_{p1}\Delta\omega$ is constant. For example, in order to compensate for a variation of the density of 40%, we need an additional damping which reduces the power by a factor of 3.

3. THE APPARATUS

3.1 General considerations

Figure 3 shows a block diagram of the apparatus. The design is largely based on well established techniques; some aspects, however, which are non conventional, are worthwhile mentioning. The low power stages use generally broadband amplification techniques with ferrite transformers. Medium and high power stages use resonant circuits with air core transformers. (Figure 4). A proper damping and a large power capability ensure the necessary bandwidth.

We already discussed the problem of bandwidth with reference to the antenna circuit. The same theory applies, but the conditions now are different. The inductance of the primary of the output transformer, L_p , is now a free parameter. The best anode load of the tubes, R , on the contrary is a given parameter, and our task is to design a circuit which charges the tubes, if possible, with this load. This can be done by properly choosing the transformer ratio and by resonating the circuit with the capacitor C_p . Now the quality factor becomes $Q=R/\omega L_p$ and following the equation (2) we find:

$$\Delta\omega = \frac{\omega^2}{R} L_p.$$

In order to obtain a large $\Delta\omega$ it might appear convenient to increase L_p . In fact a compromise must be found because of the parasitic capacity of the coil and of the decreasing coupling. If necessary, more damping is added, since the stages have a large potential power capability.

The pulsed operation mode permits a simplification of the thermal problems generally encountered in the standard c.w. technique, and with damped circuits low-loss expensive materials are no more necessary. So a careful design results in a simple construction, more economical than the usual industrial one.

3.2 The amplification chain

Consider again the simplified schematic of figure 3. The 0.5 W pilot oscillator is frequency controlled by a d.c. signal. A second signal controls the gain of a low-level amplifier. As a result we obtain a wave pulse both controlled in frequency and amplitude, able to be amplified by a linear chain.

The sequence of preamplifier, amplifier and driver results in 200 kW output to feed eight buffer power units, one for each antenna. BBC tetrodes in class B push-pull operation are used in the chain up to the 200 kW level.

3.3 Buffer power unit

Each antenna is fed by a single buffer unit using two 400 kW BBC ITK 120-2 water cooled power triodes.

These low-cost, rugged tubes for industrial heating can tolerate even a large mismatch when suitably underrated. This is indeed the case of the sixteen tubes of AFCO, which make available a total potential power of 6.4 MW. The push-pull circuit of the unit is stabilized by means of cross neutralization C_n and suitable damping resistors.

The use of a separate buffer unit for each antenna avoids any undesired coupling of the different antennae due to a common generator.

A phase shift network in the grid circuit permits an independent phase control of each antenna. A fast ignition crow-bar protects the tubes in case of arcing.

3.4 Antenna matching circuit

The design of the matching system to feed the antennae is rather unconventional in order to satisfy a number of conditions. We mention: avoid occupying space around the tokamak, provide a correct matching to a very low antenna impedance, keep the perturbation on the diagnostic equipments as low as possible and avoid ground loops in the tokamak area. Fig. 4 shows the schematic diagram of the matching circuit. L_a is the inductance of the antenna, L_t takes in account the inductance of the return path, r_a and r_{pl} are resistances representing the loss of the antenna circuit and the energy which the antenna transfer to the plasma, as already discussed in § 2.3. Note that r_{pl} increases markedly in the resonance peaks, improving the efficiency of the antenna circuit:

$$\eta_{ant} = \frac{1}{1 + \frac{r_a}{r_{pl}}} \quad (3)$$

Now consider this circuit again.

The rf cabling l is 5 m long and connects the antenna with the capacitor stack C by means of 2x18 RG 393-U 50 ohm cables. This large

number of cables connected in parallel results in a characteristic impedance of the line 1 of only 5.55Ω . Such a low impedance is necessary to reduce the circuit losses and to provide a good matching. In fact this line is connected to the capacitor C, which resonates the circuit at the frequency of operation chosen. This arrangement results in a real impedance which terminates a 100Ω , 23 m long, symmetrical line connected to the buffer unit.

Note that the impedance at the points 2-2 of figure 4, should be 100Ω for a perfect matching. In reality this condition is not always satisfied, owing to the variations of the plasma loading. Additional damping improves the matching, at the expense of the efficiency. Moreover it is evident that the condition of resonance, producing a real impedance, is only satisfied at the centre frequency. For that reason we took into account some unavoidable reflections, by convenient over-designing. An optimum design must consider all parameters in order to result in a correct load for the tubes at the points 3-3 of figure 5. Some compensation can be obtained by careful choice of the components such as the transformer, coupling capacitor, damping resistors, etc. This work was done with the help of a computer calculation following a model which considers average operating conditions.

3.5 Power supply

The buffer units are fed by capacitors storing up to 1 MJ. They are arranged in eight banks, each one feeding a single unit. This way the security is improved. When tokamak shots follow at short intervals, the residual charge in the capacitors is not lost, because the

grids of the tubes are switched in cut-off position and no current is drawn. The capacitors are designed to store twice the energy of the d.c. pulse which feeds the unit, so that AFCO has an energy source $E_0=500$ KJ available. The fractional voltage drop at the end of the pulse is $1/\sqrt{2}$. The rf output compensates for this drop using the amplitude programme.

3.6 The control of the frequency and the amplitude

AFCO can be controlled both in frequency and amplitude by suitable pre-programmes $\omega(t)$ and $A(t)$. These programmes are written before the experiment on a digitizing-pad. A digital-analogue conversion produces the signals to perform the frequency and amplitude control.

We intend to put the system in operation this way. A possible scheme for a future introduction of a frequency feedback for AFCO is the following. The rf pulse duration is divided in equal heating time intervals T_1, T_2, \dots, T_n with frequencies $\omega_1, \omega_2, \dots, \omega_n$. At the end of each heating interval a sweeping interval begins t_1, t_2, \dots, t_n , where $T \gg t$.

During the sweeping time the oscillator is swept in the interval $\omega_k - \Delta\omega_k \div \omega_k + \Delta\omega_k$ at a reduced power in order to locate the resonance peaks, and to store this information in a convenient acquisition system. By a suitable treatment of these data the next frequency ω_{k+1} is selected.

3.7 Security and monitoring

AFCO deals with a large power and therefore is provided with the usual security devices like fast crow-bar and monitoring of current, voltages, temperatures, water flow, etc. As a consequence of the large number of components, in order to make the control easier, more than 60 parameters are monitored and stored during the operation. This acquisition is local and independent of the central acquisition of TCA, to simplify the control and maintenance of AFCO. The analogue data are converted in digital form, transferred, processed and displayed by means of a small PC 100 Rainbow computer.

4. THE METHOD OF POWER MEASUREMENT

4.1 The problem

In plasma heating experiments the measurement of the power transferred from the antennae is of primary concern. It is therefore worthwhile to describe the method which will be used in order to measure the power of AFCO. This method is already currently being used in TCA.

We can in principle estimate the power absorbed by the plasma by the direct measurement of voltage, current and their phase at the antennae. This method is not easy for many reasons. The access to some antennae is indeed difficult. Moreover the measurement of the current is not straightforward because of the surface distribution of the return current and the problem of an independent calibration of the

current measuring coil. The reactive current is dominant and very low $\cos \phi$ must be measured.

4.2 Description of the method

An alternative method of measurement is therefore used which allows an easy monitoring of the antennae absorption.

Consider again the antenna circuit shown in figure 4. The method is based on the observation that the measure of the power is easier at the points 2-2, where the impedance is higher, presenting a dominant real part, the current path is well defined and the access is easy.

Consider the voltage $v=V \sin \omega t$ and the current $i=I \sin(\omega t+\phi)$ at the termination of the cables coming from the generator. The derivatives of v and i are measured by means of differential probes. An analogue treatment of these signals involving integration, phase detection, multiplication, rectification and averaging results in two d.c. signals, the first proportional to V and the second to $I \cos \phi$, which can be stored in the TCA acquisition system. The product $W=VI \cos \phi$ is the real power flowing into the circuit, and the ratio $Y=(I/V) \cos \phi$ is the real part of the admittance at the points 2-2.

The power W is the sum of the power delivered to the plasma and the power lost in the circuit

$$W = W_{pl} + W_a \quad (4)$$

Remembering now the definition of r_{pl} and r_a given previously in § 3.4, we obtain

$$W_{pl} = W \frac{r_{pl}}{r} = W \left(1 - \frac{r_a}{r}\right) \quad (5)$$

where $r = r_{pl} + r_a$.

Consider now the real admittance Y and the transmission line 1 with the characteristic impedance R_C . This line is terminated on the impedance $z = r + j\omega L$, where $L = L_a + L_t$. The classical theory of lines then applies. A simplified calculation is possible considering the following inequalities

$$\omega L \gg r ; R_C \gg z \quad (6)$$

Let us introduce now the transfer impedance of the line,

$$Z(\omega) = V/I_{ant} \quad (7)$$

where I_{ant} is the current flowing through the antenna. With these premises the following equation holds

$$Z^2 = \frac{r}{Y} \quad (8)$$

Note that in this simple model we assumed that the losses of the circuit are represented by r_a , and the equations 7 and 8 are therefore consistent with energy conservation

$$r I_{ant}^2 = V^2 Y \quad (9)$$

The equation (5) can now be rewritten as follows

$$W_{pl} = W \left(1 - \frac{Y_a}{Y}\right) \quad (10)$$

where Y_a is now the admittance in the absence of plasma, when

$r_{pl}=0$, $r=r_a$ and all the energy is dissipated in the circuit.

The practical application of this method demands a preliminary measurement without plasma giving the reference admittance Y_a . This value is stored and permits the estimation of W_{pl} using the values of W and Y measured during the tokamak discharge.

This method is valid under the assumption that L and r_a are constant. This is only approximately true, actually we did not find experimental evidence of important variation of L in the presence of plasma. The same is true for r_a , if the calibration measurement is performed in the presence of the same magnetic field as in tokamak operation. We noted indeed that the presence of this field affects r_a , presumably by a variation of the skin depth.

4.3 Errors and calibration

We make a few remarks about the precision of this method. From equation (10) we note that the power delivered to the plasma is deduced from measurements of voltage and current in a single place and do not depend on Z . For that reason the precision of the measurement of I_{ant} and r resulting from the more or less accurate estimation of Z do not affect the measurement of the power. The calibration of the system is straightforward. The circuit is open at points 2-2 and charged with calibrated resistances. The power is then deduced from the measurement of the voltage across the resistance.

5. SOME PRELIMINARY TEST

A preliminary test of AFCO was made checking the pilot and pre-amplifier, the amplification chain and one buffer unit. An estimation of the output power was made on a dummy load, and pulses of 300 KW, 120 ms were produced at 0.5, 2.5 and 5 MHz. Furthermore some checks were carried out using a circuit simulating the antenna.

The system works as expected and we are starting to set up AFCO for service in the TCA experiment.

6. EFFICIENCY AND POWER

Efficiency is a major concern of heating techniques. We wish to close this paper with some technical considerations about AWH, comparing TCA with large size tokamaks.

6.1 Efficiency of AFCO

Firstly note that AFCO is not aimed to optimize the efficiency, it is conceived rather as a device which provides the best conditions for varying experimental conditions. In this way all the data which will be necessary for a further optimisation of the efficiency will be collected. We think it is nevertheless useful to give a brief presentation of the expected performance of AFCO in TCA.

Let us firstly define the total efficiency η_{tot} as the ratio of

the energy coupled to the plasma with the d.c. energy source, which was discussed in § 3.5.

It is useful to split η_{tot} in two terms

$$\eta_{\text{tot}} = \eta_g \eta_{\text{ant}} \quad (11)$$

where η_{ant} is the efficiency of the antenna circuit, given by (3) in § 3.4, and η_g is the efficiency of the generator up to the antenna circuit.

Figure 5 shows an estimation of the efficiency of AFCO as a function of the frequency under the following assumptions:

- 1) We consider the "standard" plasma coupling (§ 2.2), $r_{\text{pl}}=r_0$, following the measurement at 2.5 MHz and a proportional dependence on the frequency, in agreement with theory and preliminary experience.
- 2) The skin effect was considered to estimate the frequency dependence of the circuit loss.
- 3) AFCO operates at constant frequency.
- 4) The efficiency of the generator η_g was computed using the known technical rules, in agreement with the test reported in § 5.

The estimation of the efficiency when AFCO operates at variable frequency is more difficult. In fact, following the basic principle exposed in § 2.4, a decrease of the efficiency is expected due to the damping. We note, however, that we can hope to follow some resonance,

when the frequency control is in action, increasing the efficiency. The two effects may balance partially.

6.2 Heating power

The expected average power which AFCO will transfer to the plasma results from the estimated efficiency η , when we consider the energy of the source E_0 and the length of the pulse, τ :

$$\langle W_{pl} \rangle = \eta E_0 / \tau \quad (12)$$

For example let us calculate $\langle W_{pl} \rangle$, with the help of figure 5, at the frequency of 2.5 MHz and for a duration τ of 120 ms. Remembering that, from § 3.5, $E_0 = 500$ kJ, we get $\langle W_{pl} \rangle = 1$ MW. This estimation is coherent with the result of the preliminary test (§ 5).

Note that AFCO can produce more power if the pulse duration is reduced. In this case the potential power of the generator must be taken in account, following § 3.3.

The same argument, and that one discussed in § 2.3, can help us to estimate the operation at variable frequency. In heating experiments it is usual to compare the additional heating power with the ohmic power of the tokamak discharge, which in TCA goes up to about 250 KW. We are therefore confident that AFCO will deliver enough power for doing meaningful experiments in TCA.

7. AWH IN LARGE SIZE TOKAMAKS

We limit the discussion to a few technical remarks. The increase in the time scale of the big experiments can allow a mechanical tuning of resonant circuits. Then the additional damping is no more necessary, and the efficiency is improved. The antenna circuit is a very important part of the apparatus, if we consider efficiency. Looking at equation (3) of § 3.4, we can ask how the ratio r_a/r_{p1} will change with the size of the experiment. In an ad hoc planned experiment, one can try to place the resonating capacitors in the proximity of the antennae to decrease r_a . Note that AWH allows the generator to be placed far from the tokamak, if a proper matching is done near the antennae. It is difficult to give now a definite answer concerning the plasma coupling r_{p1} , owing to the large variations of this quantity in various experimental conditions. We hope that AFCO will help to answering this question by the future experimental programme of TCA.

ACKNOWLEDGEMENTS

The authors gratefully acknowledge the valuable help of Mr. I. Kjelberg concerning the transfer of the control signals to the local computer, and of Mr. P. Marmillod concerning the analogue treatment of the data for the measurement of the power. Thanks are due to Dr. G. Collins, who wrote the programme for the acquisition and analysis of these data, and to Dr. J.B. Lister for reading the manuscript and for useful discussions.

REFERENCES

Appert K, Gruber R, Troyon F and Vaclavik J 1982 Excitation of global eigenmode of the Alfvén wave in Tokamaks

Plasma Phys. 24 1147-1159

Collins GA et al. 1985 Measurements of the Alfvén wave spectrum in TCA Laboratory Report LRP 265/85

Ecole Polytechnique Fédérale de Lausanne, CRPP, Lausanne-Switzerland

De Chambrier A et al. 1982a The technique of Alfvén wave heating in the TCA Tokamak

12th Symposium on Fusion Technology, Aachen, proceedings 1295-1300

De Chambrier A et al. 1982b Alfvén wave coupling experiment on the TCA Tokamak

Plasma Phys. 24 893-902

Lietti A et al. 1981 The R.F. system for Alfvén wave heating of the TCA Tokamak

9th Symposium on Engineering Problems of Fusion Research, Chicago, proceedings 835-838

LIST OF CAPTIONS FOR ILLUSTRATIONS

Figure 1. Loading spectrum with various excitation modes; (a) 2.1;
(b) 1,1; (c) 2.0.

Figure 2. Antennae arrangement.
+ phase connection for the $n=2, |m|=1$ mode.

Figure 3. A block diagram of the apparatus.

Figure 4. Schematic diagram of the buffer unit and of the antenna
matching circuit.

Figure 5. Efficiency of the heating in the continuum.

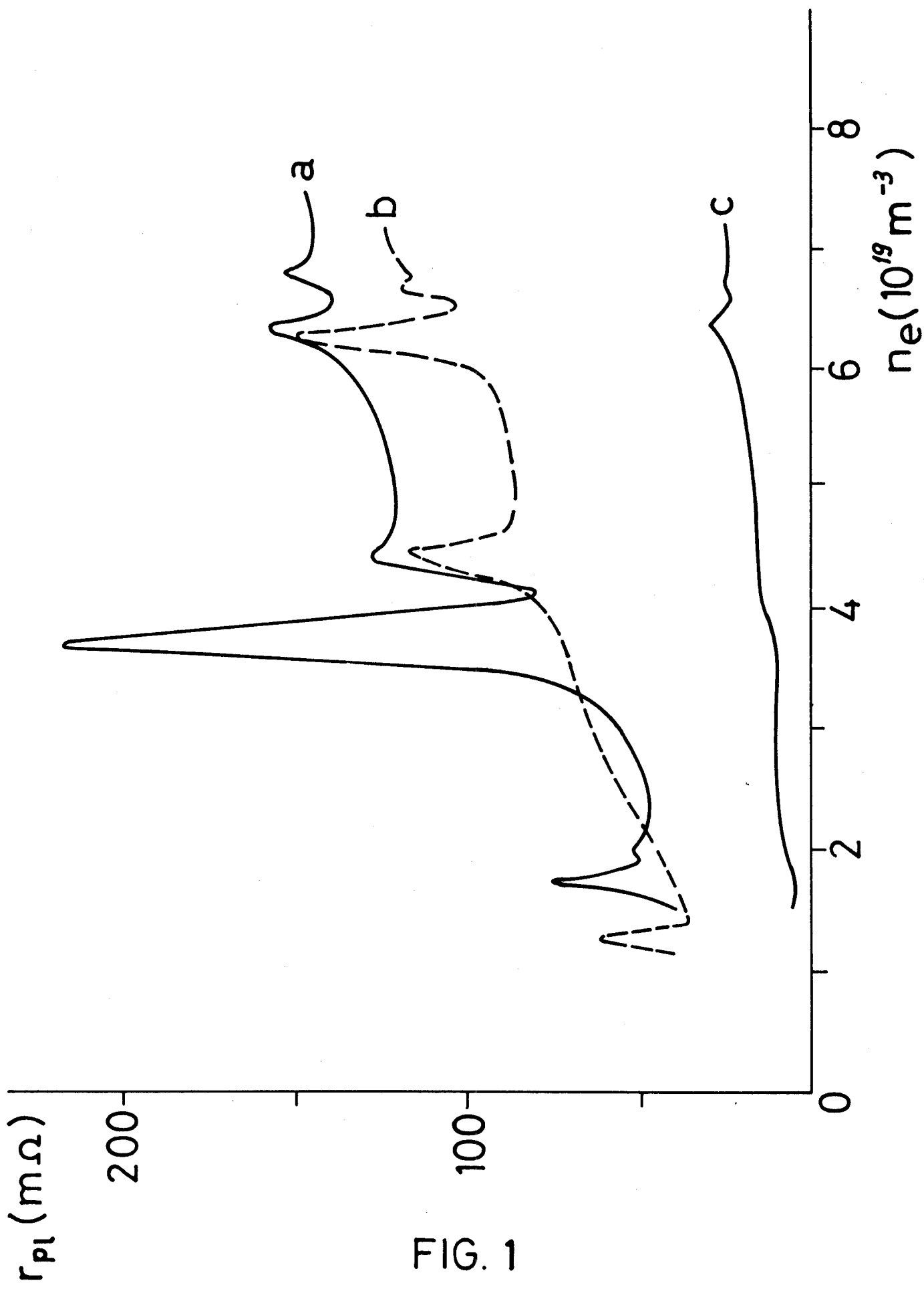
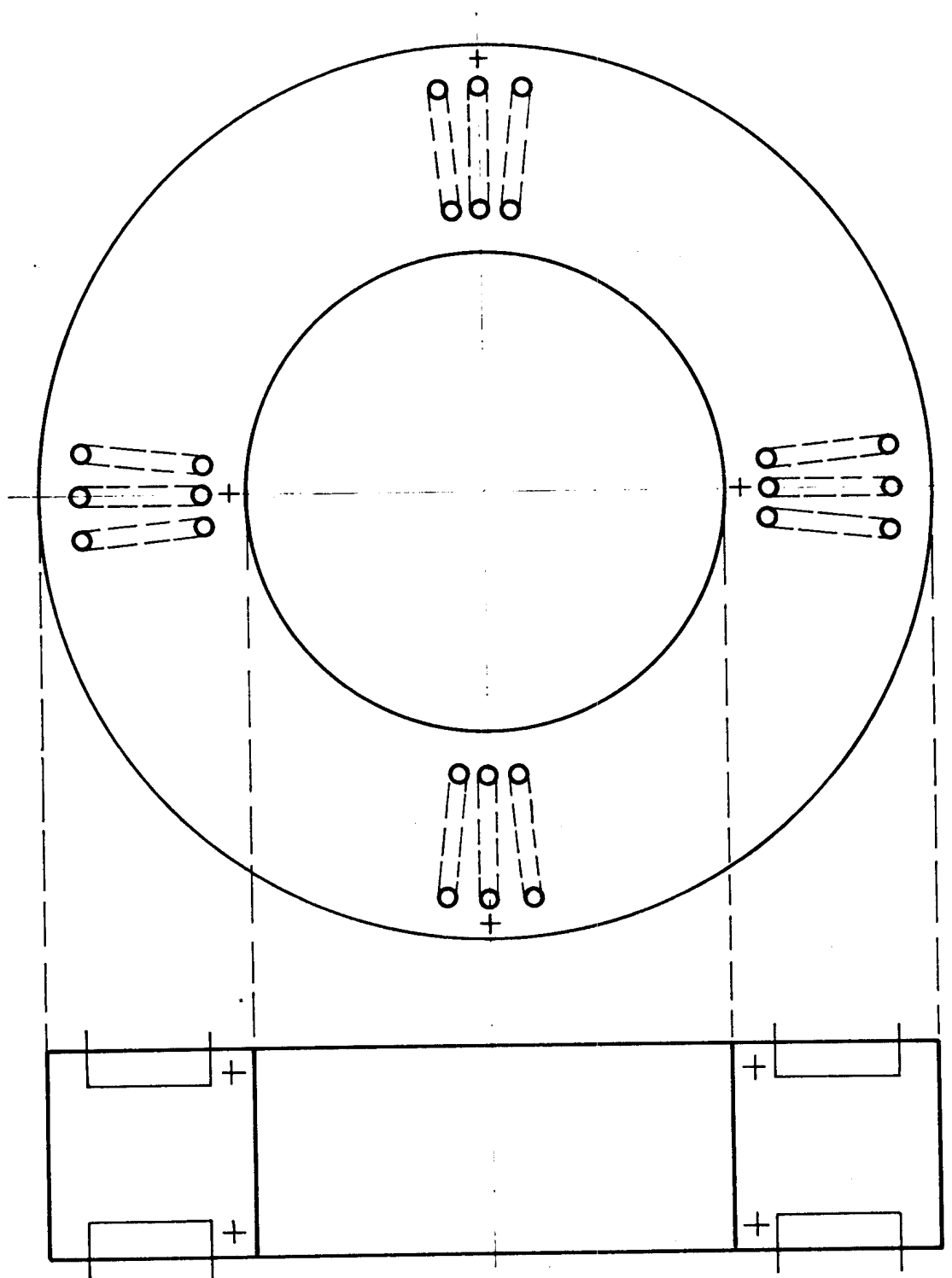


FIG. 1



Antennae arrangement
 + phase connection for the $n=2, |m|=1$ mode

Fig. 2

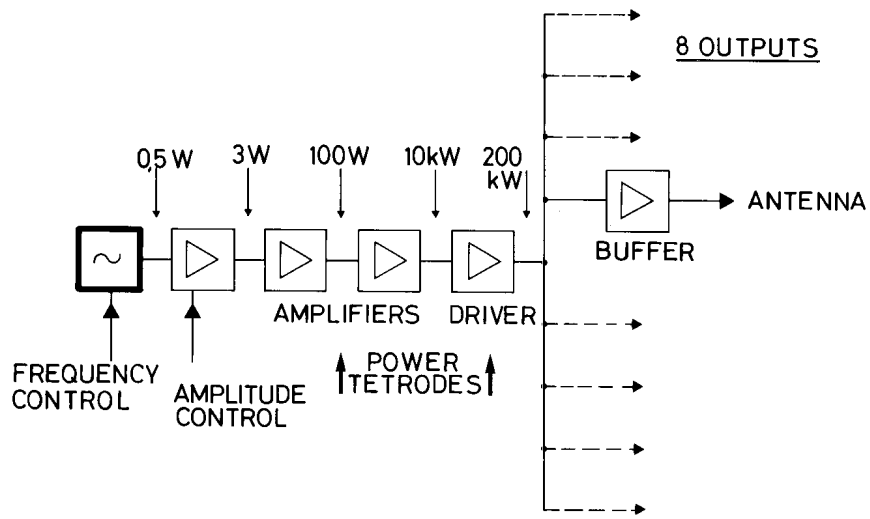


Fig. 3

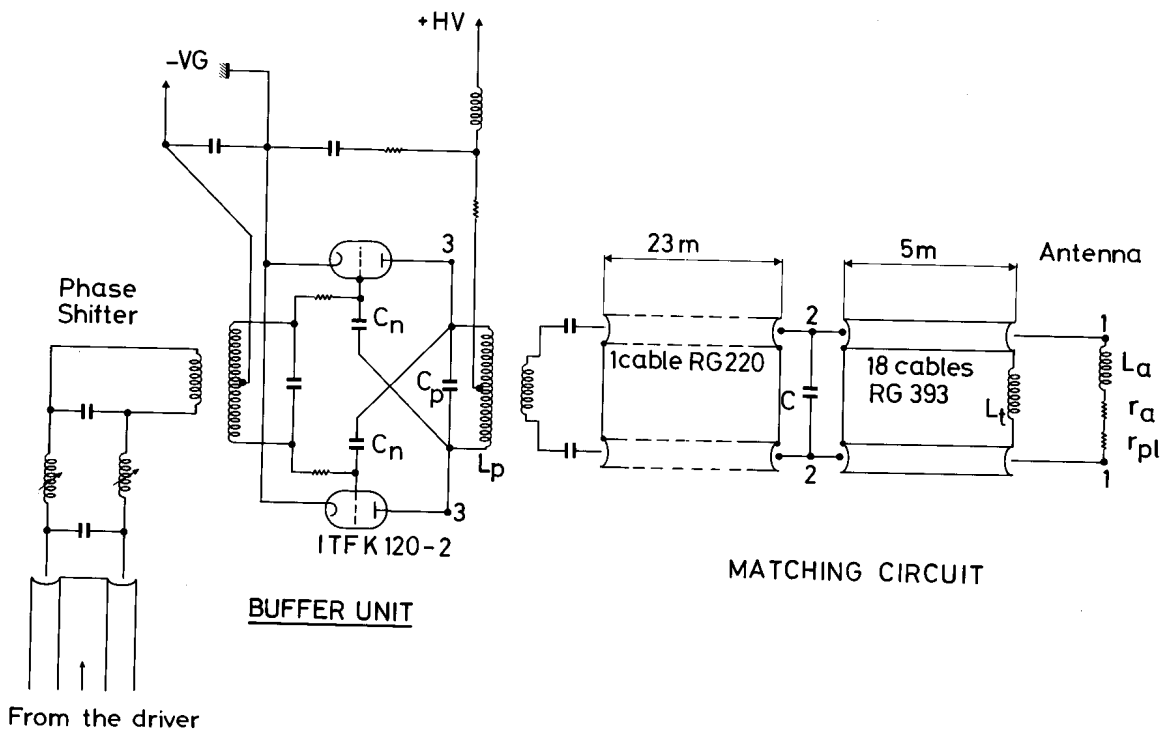


Fig. 4

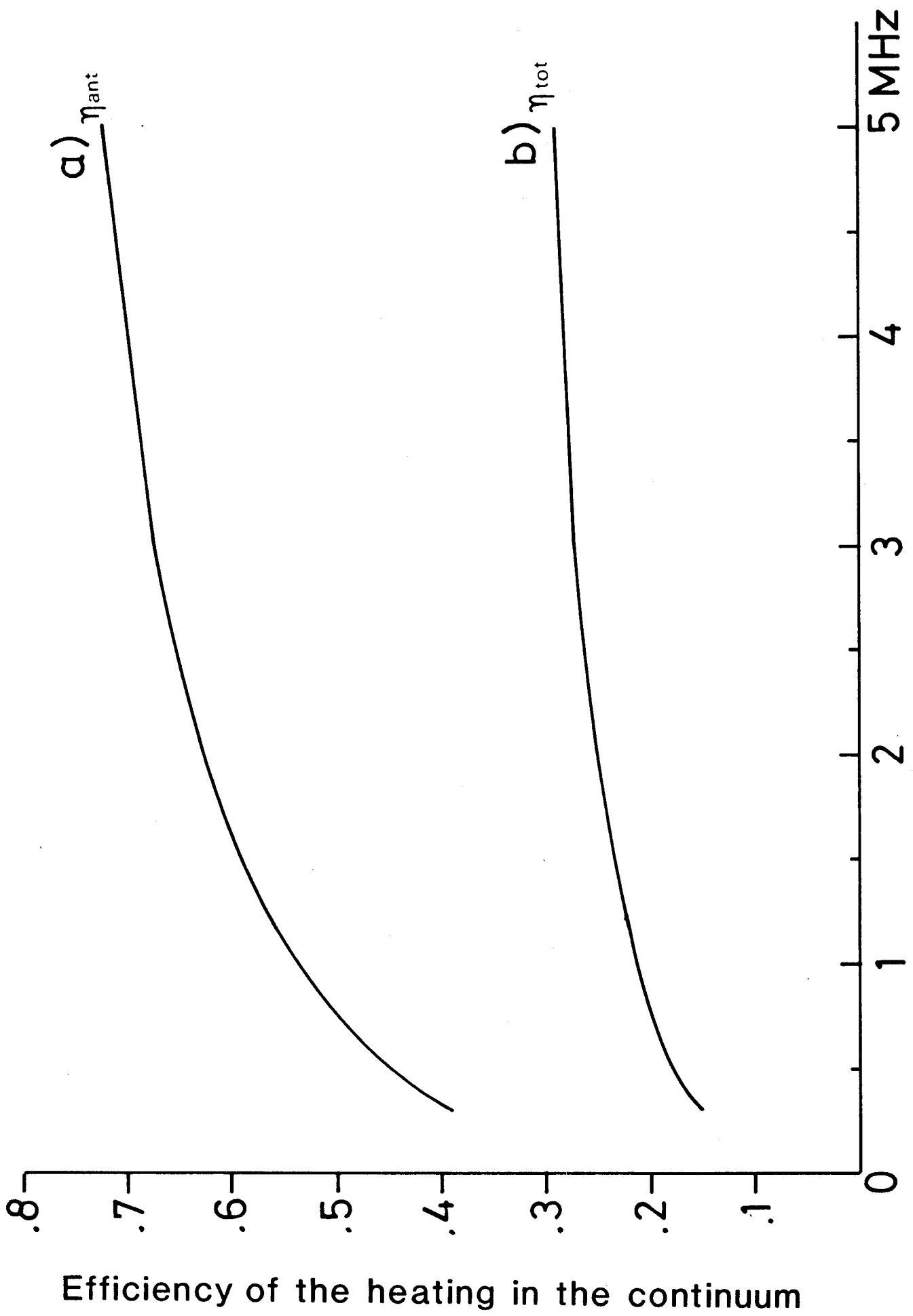


Fig. 5